Differential Recognition of the Free versus Bound Retinol by Human Microsomal Retinol/Sterol Dehydrogenases: Characterization of the Holo-CRBP Dehydrogenase Activity of RoDH-4[†]

Elena A. Lapshina,[‡] Olga V. Belyaeva, Olga V. Chumakova, and Natalia Y. Kedishvili*

Division of Molecular Biology and Biochemistry, School of Biological Sciences, University of Missouri−Kansas City, Kansas City, Missouri 64110

Received September 11, 2002; Revised Manuscript Received November 25, 2002

ABSTRACT: All-*trans*-retinol is the precursor for all-*trans*-retinoic acid, the activating ligand for nuclear transcription factors retinoic acid receptors. In the cytosol of various cells, most retinol exists in a bound form, complexed with cellular retinol binding protein type I (holo-CRBP). Whether retinoic acid is produced from the free or bound form of retinol is not yet clear. Here, we present evidence that holo-CRBP is recognized as substrate by human microsomal short-chain dehydrogenase/reductase (SDR) RoDH-4 with the K_m value close to the liver concentration of holo-CRBP. The ability to utilize holo-CRBP differentiates RoDH-4 from a related enzyme, RoDH-like 3α-hydroxysteroid dehydrogenase (3α-HSD), which is 3-fold more active with free retinol than RoDH-4 but is 15-fold less active toward holo-CRBP. Recognition of the cytosolic holo-CRBP as substrate is consistent with RoDH-4 orientation in the membrane. As established by immunoprecipitation and glycosylation scanning, RoDH-4 faces the cytosolic side of the membrane. Purified RoDH-4, stabilized by reconstitution into proteoliposomes, exhibits the apparent K_m values for substrates and NAD^+ similar to those of the microsomal enzyme and oxidizes holo-CRBP with the catalytic efficiency (k_{cat}/K_m) of 59 min^{-1} mM^{-1}. Apo-CRBP acts as a strong competitive inhibitor of holo-CRBP oxidation with an apparent K_i value of 0.2 μM. The results of this study suggest that the human retinol-active SDRs are not functionally equivalent and that, in contrast to RoDH-like 3α-HSD, RoDH-4 can access the bound form of retinol for retinoic acid production and is regulated by the apo-/holo-CRBP ratio.

All-*trans*-retinol is the precursor for all-*trans*-retinoic acid, which serves as an activating ligand for a family of nuclear retinoic acid receptors (RARs) (reviewed in ref *1*). RARs regulate gene transcription during embryogenesis and in adulthood (reviewed in ref *2*). All-*trans*-retinoic acid is produced from all-*trans*-retinol in two oxidative steps: retinol is oxidized to retinaldehyde and then further to retinoic acid (*3*). In the cytosol of most cells retinol is complexed with one of the four cellular retinol binding proteins (CRBPs).[1] CRBP type I is the most widespread retinol binding protein, which exhibits a somewhat different distribution pattern in rat versus human tissues (reviewed in ref *4*). The expression pattern of other retinol binding proteins appears to be more restricted. CRBP type II is expressed in the small intestine (*4*), human CRBP type III is abundant in kidney and liver (*5*), murine CRBP type III is expressed in heart, skeletal muscle, adipose tissue, and mammary gland (*6*), and human CRBP type IV is present in kidney, heart, and colon (*7*). Binding to CRBPs, especially to CRBP type I ($K_d \sim 0.1$ nM), lowers the concentration of free retinol in the liver cytosol to less than 0.002 μM (reviewed in ref *8*). In contrast, the concentration of the CRBPI-bound retinol (holo-CRBP) in liver is ∼5 μM (*8*). Thus, in tissues with a high level of CRBP expression, holo-CRBP is the predominant form of retinol.

Partial purification and characterization of the first holo-CRBP dehydrogenase, RoDH-1, from rat liver microsomes provided evidence that the bound form of retinol can be oxidized (*9*). Cloning of the corresponding cDNA revealed that RoDH-1 belongs to the superfamily of short-chain dehydrogenases/reductases (SDR) (*10*), which also includes steroid and prostaglandin dehydrogenases. The partially purified RoDH-1 was shown to oxidize holo-CRBP with apparent K_m and V_{max} values of 0.6−1.6 μM and ∼0.105 nmol min^{-1} mg^{-1}, respectively, in the presence of $NADP^+$ as the preferred cofactor (*9*). However, the true catalytic efficiency of this enzyme remains unknown, because the solubilized enzyme is quite unstable and loses activity during purification. The partially purified preparation of RoDH-1 contained an additional protein band of ∼54 kDa, which

[†] Supported by the National Institute on Alcohol Abuse and Alcoholism Grants AA00221 and AA12153 to N.Y.K.

* To whom correspondence should be addressed. Phone: (816) 235-2658. Fax: (816) 235-5595. E-mail: kedishvilin@umkc.edu.

[‡] Present address: Institute of Biochemistry, Len. Kom. Blvd., 50, Grodno, Belarus 230017.

[1] Abbreviations: CRBP, cellular retinol binding protein; holo-CRBP, CRBP type I saturated with all-*trans*-retinol; SDR, short-chain dehydrogenase/reductase; RoDH, retinol dehydrogenase; 3α-HSD, 3α-hydroxysteroid dehydrogenase; 11β-HSD1, 11β-hydroxysteroid dehydrogenase type 1; SDS−PAGE, polyacrylamide gel electrophoresis in the presence of sodium dodecyl sulfate; hCE-1, human carboxylesterase type 1; PMSF, phenylmethanesulfonyl fluoride; Endo H, endoglycosidase H; DHPC, 1,2-diheptanoyl-*sn*-glycero-3-phosphocholine; ER, endoplasmic reticulum; PBS, phosphate-buffered saline; ADH, alcohol dehydrogenase; ALDH, aldehyde dehydrogenase; ARAT, acyl-CoA: retinol acyltransferase; LRAT, lecithin−retinol acyltransferase.

10.1021/bi026836r CCC: $25.00
Published on Web 12/31/2002

appeared to copurify with RoDH-1 and could be required for its activity toward holo-CRBP. Subsequently, a second holo-CRBP dehydrogenase, RoDH-2, was cloned from rat liver (*11*). RoDH-2 oxidized holo-CRBP with an apparent K_m value of 2 μM and, similar to RoDH-1, exhibited preference for $NADP^+$ as cofactor (*11*). In addition to retinoids, both RoDH-1 and RoDH-2 were shown to recognize 3α-hydroxysteroids as substrates (*12*, *13*).

Search for the human homologues of rat RoDH enzymes identified two human SDRs active toward all-*trans*-retinol and 3α-hydroxysteroids, RoDH-4 (also called hRDH-E) (*14*, *15*) and RoDH-like 3α-hydroxysteroid dehydrogenase (3α-HSD) (*12*, *16*). Unlike the rat enzymes, human retinol/sterol dehydrogenases preferred NAD^+ over $NADP^+$ as cofactor. Previous analysis suggested that RoDH-like 3α-HSD did not recognize holo-CRBP as substrate (*16*). To determine whether RoDH-4 could play a role in the metabolism of bound retinol in human tissues, we characterized RoDH-4 activity toward holo-CRBP in the present study, using RoDH-like 3α-HSD as a negative control for oxidation of holo-CRBP.

EXPERIMENTAL PROCEDURES

Construction of Plasmids and Expression in Insect Sf9 Cells. The baculovirus expression constructs for RoDH-4 and RoDH-like 3α-HSD were described previously (*14*, *16*). The expression levels of both proteins in Sf9 cells were similar. Additional constructs of RoDH-4 containing artificially introduced glycosylation sites for analysis of membrane orientation were prepared by site-directed mutagenesis using an ExSite PCR-based kit (Stratagene, La Jolla, CA). The glycosylation site at position 60 was created by converting Cys-60 to Asn using oligonucleotide primers TGC TGG CTG CAA ATC TGA CGG AGA A (sense) and CCC GCA AGC CTC GTG CAT CC (antisense). The glycosylation site at position 124 was introduced by substitution of Leu-124 for Asn using primers GGC TCC CAA TGA GAA TCT CAC CAA GCA GG (sense) and GTG GGC AAG GAG ATG CCA GCA T (antisense). Finally, Asp-260 was converted to Asn using primers AGT GCA CAC AGA ATC TGT CGT TGG (sense) and TCTGCT CCA TTT GTT CAG CTG ATT T (antisense). The mismatched bases in the sense primers are underlined. The full-length coding sequence for 11β-hydroxysteroid dehydrogenase type 1 (11β-HSD1), which was used as a control protein to monitor glycosylation efficiency of Sf9 cells, was amplified using the sense primer GCT GGA TCC GCC ATG GCT TTT ATG AAA AAA TAT CTC (*Bam*HI site underlined) and the antisense primer AGG TCT AGA CTA GTC GTC GTC GTC CTT GTA GTC CAT CTT GTT TAT GAA TCT GTC CAT ATT ATA GC (*Xba*I site underlined), which encoded the FLAG epitope MDYKDDDD. The product was cleaved with *Bam*HI and *Xba*I restriction endonucleases and cloned into the baculovirus transfer vector pVL1393.

All constructs were verified by sequencing and expressed in insect Sf9 cells using the BaculoGold baculovirus system.

For in vitro protein synthesis, some RoDH-4 constructs were cloned into *Bam*HI/*Eco*RI restriction sites of expression vector pT7/T3-19 (Ambion Inc., Austin, TX). The expression construct for 11β-hydroxysteroid dehydrogenase type 1 (11β-HSD1) was described previously (*17*). ^{35}S-Labeled RoDH-4 and 11β-HSD1 proteins were produced in vitro using the TNT Quick system and dog pancreas microsomes (Promega) and subjected to 12% denaturing polyacrylamide gel electrophoresis in the presence of sodium dodecyl sulfate (SDS−PAGE) (*17*). The protein bands were visualized by autoradiography.

Isolation of Microsomes and Preparation of Holo-CRBP. Sf9 cells were collected by centrifugation at 5000*g* for 10 min and homogenized using a French pressure minicell at 800 psig. Microsomes were isolated from the post-12000*g* supernatant by centrifugation at 105000*g* for 2 h through a 0.6 M sucrose cushion and resuspended in 0.1 M potassium phosphate, pH 7.4, 0.1 mM EDTA, 1 mM DTT, and 20% glycerol. Protein concentrations were determined by Lowry (*18*).

CRBP was expressed in *Escherichia coli* as a fusion protein with glutathione *S*-transferase and purified using affinity chromatography on a glutathione−agarose column (*19*). The fusion protein was cleaved with thrombin, and CRBP was separated from glutathione *S*-transferase on a Q-Sepharose column (*19*). To prepare holo-CRBP, apo-CRBP was incubated with a 2-fold molar excess of all-*trans*-retinol for 1 h in the dark, and the excess of free all-*trans*-retinol was removed by gel filtration through a G-50 Sephadex column (2.6 cm × 30 cm). The A_{350}/A_{280} ratio of the holo-CRBP preparation was 1.6−1.7.

Activity Assays and Determination of Kinetic Constants. Activity assays were performed in 90 mM potassium phosphate, pH 7.3, and 40 mM KCl at 37 °C in siliconized glass tubes (*14*). Retinol dehydrogenase activity was determined using free retinol or holo-CRBP in the presence of 1 mM NAD^+ as cofactor (*14*, *16*). In some experiments, retinaldehyde was converted into retinaldehyde oximes by the addition of cold 2 M hydroxylamine−bicarbonate buffer, pH 6.5, according to the published protocol (*20*).

Initial velocities of holo-CRBP oxidation (nanomoles per minute per milligram) were determined at fixed saturating 1 mM NAD^+ and seven concentrations of holo-CRBP ranging from 1.25 to 17.5 μM. The reactions were carried out for 20 min with 5.5 μg/mL RoDH-4 microsomes or with 0.625 μg/mL purified RoDH-4 reconstituted into proteoliposomes. Under these conditions, the reaction rate was linearly proportional to the reaction time and protein concentration, and the amount of product was less than 10% of the substrate. The background levels of retinaldehyde or retinaldehyde oxime with holo-CRBP as substrate in the absence of cofactor were negligible. The background levels of retinaldehyde with free retinol in the absence of cofactor were at least 3-fold lower than in the presence of cofactor and were subtracted from each experimental data point. The apparent K_m and V_{max} values were determined from nonlinear regression fit of enzyme kinetic data to the Michaelis−Menten equation using the GraFit software package.

Apo-CRBP inhibition of holo-CRBP oxidation was evaluated by incubating RoDH-4-containing proteoliposomes with 1 mM NAD^+, four to six concentrations of holo-CRBP (1.25−15 μM), and three concentrations of apo-CRBP (0.6−3.0 μM). Each data set was evaluated for fit to different types of inhibition (*21*) using the method of Marquart (*22*).

The 3α-HSD activity of RoDH-4 was assayed using tritiated androsterone in the presence of NAD^+ as cofactor (*14*). Steroid reaction products were analyzed by thin-layer

chromatography. The apparent K_m value of RoDH-4 for androsterone was determined using six concentrations of androsterone (0.05−1 μM) in the presence of saturating NAD^+ (1 mM). The apparent K_m value for NAD^+ was determined using six concentrations of NAD^+ (0.05−6.4 μM) in the presence of a fixed concentration of androsterone (1 μM).

For the membrane orientation studies, proteoliposomes and Sf9 microsomes containing RoDH-4 were incubated with a pore-forming antibiotic alamethicin (50 μg/mg of protein) on ice for 15 min (*23*). In one set of assays, permeabilized proteoliposomes and microsomes were preincubated with 1 mM NAD^+ before the addition of 0.5 μM androsterone to the reaction mixture. In another set of assays, NAD^+ was added the last. There was no difference in the reaction rates between the two sets of experiments. The control reactions were performed without the cofactor. Reaction products were analyzed by thin-layer chromatography as described above.

Alkaline Extraction, Protease Resistance Assays, and Endoglycosidase H Treatment. For alkaline extractions, human liver microsomes (Human Cell Culture Center, Inc., Laurel, MD) or Sf9 microsomes (10 μg in 5 μL) were diluted with 100 μL of 100 mM sodium carbonate (pH 11.5) and 25 mM potassium acetate or with 100 μL of 1% Triton X-100 in PBS and incubated for 30 min on ice. Samples were layered over a 100 μL cushion of 0.5 M sucrose prepared in alkaline or detergent-containing extraction buffer and centrifuged at 200000*g* for 1 h. Pellets were dissolved in 20 μL of SDS−PAGE loading buffer and denatured by heating. Supernatants were precipitated with an equal volume of ice-cold 50% trichloroacetic acid for 30 min on ice and centrifuged for 3 min at 12000*g* at 4 °C. The resulting pellets were washed twice with ethyl ether, dried, and dissolved in 20 μL of SDS−PAGE loading buffer. Following separation in 12% SDS−PAGE, samples were transferred to Hybond-P membrane (Amersham Pharmacia Biotech), and RoDH-4 was detected using the ECL western blotting analysis system and Hyperfilm ECL (Amersham Pharmacia Biotech). Rabbit polyclonal antibodies against the C-terminal fragment of RoDH-4 were used at a 1: 5000 dilution (*14*). Polyclonal antibodies against the human carboxylesterase 1 (hCE-1) (*24*), which served as a positive control for extraction of microsomal proteins, were kindly provided by Dr. William Bosron (Indiana University School of Medicine) and were used at a 1:10000 dilution.

For protease resistance studies, human liver microsomes or Sf9 microsomes were incubated with proteinase K (Roche Molecular Biochemicals) at a 10:1 (μg/μg) ratio for 1 h at 4 °C or for 1 h at 37 °C in the presence or absence of 1% Triton X-100. Similarly, proteins synthesized in vitro using the TNT Quick system were incubated with 200 μg/mL proteinase K at 4 °C for 1 h in the presence or absence of 1% Triton X-100. The reactions were stopped by the addition of phenylmethanesulfonyl fluoride (PMSF) to the final concentration of 4 mM. Samples were denatured using SDS−PAGE loading buffer, separated in 12% SDS−PAGE, and analyzed either by autoradiography or by western blotting as indicated.

For endoglycosidase H (Endo H) treatment, 20 μg of microsomal protein was resuspended in 50 mM sodium phosphate buffer, pH 5.5, containing 0.1% SDS and 0.1 M 2-mercaptoethanol. PMSF was added to the final concentration of 5 mM. One-half of the mixture was treated with 2.5 μL (12.5 units) of Endo H (Boehringer Mannheim) and the other half received 2.5 μL of the buffer. Both samples were incubated overnight at room temperature, then denatured with SDS−PAGE loading buffer for 5 min at 94 °C, and analyzed by western blotting.

Immunoprecipitation. The IgG fractions of rabbit polyclonal antisera against the N-terminal (residues 22−104) and the C-terminal (residues 159−304) segments of RoDH-4 (*14*) were purified by affinity chromatography on ImmunoPure immobilized protein A gel according to the supplier's recommendations (Pierce Chemical Co., Rockford, IL). The purity of the IgG fractions was evaluated by SDS−PAGE and Coomassie Blue staining. For immunoprecipitation studies, intact microsomal vesicles containing RoDH-4 were incubated with indicated amounts of immune or preimmune IgG at 4 °C overnight. The samples were then incubated with protein A−agarose beads at 4 °C for another 24 h and centrifuged for 5 min at 5000*g*. Supernatants were precipitated with an equal volume of ice-cold 50% TCA, washed twice with ethyl ether, dried, and dissolved in SDS−PAGE loading buffer. Protein A-bound immune complexes were eluted with the ImmunoPure elution buffer for immobilized protein A (Pierce), neutralized with the binding buffer, and denatured using SDS−PAGE loading buffer. SDS−PAGE and western blotting were performed as described above.

Purification and Reconstitution into Proteoliposomes. Solubilization of microsomal membranes was performed using 1,2-diheptanoyl-*sn*-glycero-3-phosphocholine (DHPC) (Avanti Polar Lipids, Alabaster, AL) (*25*). A freshly thawed suspension of microsomal membranes containing RoDH-4 was diluted with 100 mM potassium phosphate, 150 mM KCl, 20% (w/v) glycerol, 0.1 mM EDTA, and 1 mM DTT, pH 7.4, to a final protein concentration of 3.5 mg/mL. Membranes were solubilized at 4 °C by adding a 200 mM stock solution of DHPC in the above buffer dropwise under vortexing to a final concentration of DHPC of 15 mM. The membrane suspension was vortexed for another 30 min and centrifuged at 100000*g* and 4 °C for 1 h (Beckman Optima LE-80K ultracentrifuge, rotor SW 55Ti). The extraction efficiency and the enzyme stability at various stages were monitored following the 3α-HSD activity of RoDH-4. The DHPC extract was stable for several months without apparent loss of activity if stored in aliquots at −80 °C in potassium phosphate buffer with 20% glycerol.

For purification and reconstitution of RoDH-4 into proteoliposomes, DHPC extract was incubated with proteinase K at a 10:1 (μg/μg) ratio for 14 h on ice. At the end of the incubation, proteinase K was inactivated by the addition of PMSF dissolved in ethanol to the final concentration of 4 mM, followed by incubation on ice for 1 h. Proteinase K-treated extract (~300 μL) was reconstituted into artificial lipid membrane in the presence of DHPC. For vesicle preparation, 100 μL of a 3 mM premixed lipid solution of egg yolk L-α-phosphatidylcholine and dipalmitoyl-DL-α-phosphatidyl-L-serine at a 85:15 molar ratio in chloroform−methanol (9:1 v/v) was dried down in 16 × 110 mm glass test tubes under a gentle stream of nitrogen for 2.5 h. RoDH-4-containing vesicles were prepared by dissolving the lipid film in proteinase K-treated extract. The lipids were dissolved by gentle agitation for 15 min at room temperature. Vesicles were then formed from these samples by rapid dilution

followed by extensive dialysis as follows. While vortexing vigorously, 3 mL of reconstitution buffer (at room temperature) was added to the sample, thereby diluting the detergent below its critical micellar concentration (10-fold), promoting vesicle formation. Then, the detergent was removed by dialysis (in Spectrapore 6−8 kDa cutoff dialysis tubing) against 4 L of reconstitution buffer (10 mM potassium phosphate, 100 mM potassium chloride, 10% glycerol, 1 mM DTT, pH 7.4) containing 4 g of Bio-Beads SM2 beads (Bio-Rad) at 4 °C overnight with no buffer changes. Vesicles were recovered and concentrated by flotation in a Nycodenz (Sigma) step gradient (*26*). Fractions of dialysate (1.5 mL) were mixed with 1.5 mL of 80% Nycodenz (w/v) dissolved in reconstitution buffer in 5 mL of Beckman ultracentrifuge tubes and overlaid with 750 μL of 30% Nycodenz in reconstitution buffer followed by 500 μL of reconstitution buffer lacking glycerol. The samples were centrifuged in a SW 55Ti rotor (Beckman) for 6 h at 52000 rpm at 4 °C. RoDH-4-containing vesicles were harvested from the 0/30% Nycodenz interface and combined. The vesicles were stored at 4 °C without apparent loss of activity for at least 4 months.

RESULTS

RoDH-4 but Not RoDH-like 3α-HSD Is Active toward Holo-CRBP. To compare the retinol dehydrogenase activities of human RoDH-4 and RoDH-like 3α-HSD, we expressed the corresponding cDNAs in Sf9 cells and isolated the microsomal membranes. The recombinant proteins appeared as distinct protein bands in the microsomal fraction of Sf9 cells after electrophoretic separation in denaturing polyacrylamide gel and staining with Coomassie Blue R-250. The expression levels of RoDH-4 and RoDH-like 3α-HSD in Sf9 microsomes were similar (data not shown). The identity of the bands was confirmed by western blotting as described previously (*14*, *16*).

Retinol dehydrogenase activity of the microsomes was assayed using 5 μM free retinol or 5 μM holo-CRBP. The products were analyzed by normal-phase HPLC as described under Experimental Procedures. RoDH-4 microsomes were ~3-fold less active with free retinol than RoDH-like 3α-HSD microsomes (0.4 versus 1.3 nmol min^{-1} mg^{-1}) (Figure 1, open bars). At the same time, RoDH-4 microsomes were ~15-fold more active with 5 μM holo-CRBP than RoDH-like 3α-HSD microsomes (0.23 versus ~0.015 nmol min^{-1} mg^{-1}) (Figure 1, shaded bars). The activity of RoDH-like 3α-HSD microsomes with holo-CRBP was only slightly higher than that of the control microsomes (~0.013 nmol min^{-1} mg^{-1}) that were isolated from Sf9 cells infected with wild-type virus and which, therefore, did not contain RoDH proteins. Thus, although RoDH-like 3α-HSD was more active than RoDH-4 with free retinol, RoDH-4 was more active with holo-CRBP. Oxidation of holo-CRBP by RoDH-4 followed Michaelis−Menten kinetics with apparent K_m and V_{max} values of 3.8 ± 0.8 μM and 390 ± 30 pmol min^{-1} mg^{-1} microsomal protein, respectively (Figure 2).

Membrane Orientation of RoDH-4 Is Consistent with Its Binding of Holo-CRBP. Since the activity assays suggested that RoDH-4 recognized holo-CRBP as substrate, we were interested in whether the microsomal RoDH-4 could physically interact with the cytosolic holo-CRBP. To determine

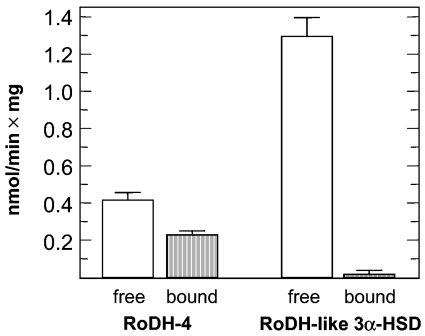

FIGURE 1: Activity of RoDH-4 and RoDH-like 3α-HSD toward free and CRBP-bound all-*trans*-retinol. Microsomal preparations containing RoDH-4 and RoDH-like 3α-HSD were used at a concentration of 5.5 μg/mL. The final concentration of holo-CRBP and free retinol in the reaction mixture was 5 μM. The reactions were carried out for 30 min at 37 °C, and the products were extracted and analyzed by HPLC as described under Experimental Procedures. The results shown are the mean ± SD of three independent experiments.

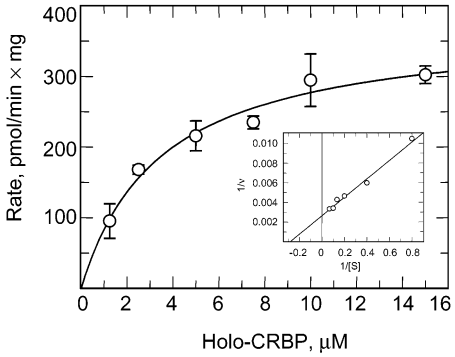

FIGURE 2: Determination of kinetic constants for oxidation of holo-CRBP by microsomal RoDH-4. The reactions were carried out as described in Figure 1. The concentration of NAD^+ was 1 mM. Kinetic constants were calculated using GraFit (Erithacus Software Ltd.). Reported values are the averages from four experiments, with the standard deviations indicated.

whether RoDH-4 was an integral or a peripheral membrane protein, we incubated human liver microsomes in sodium carbonate (pH 11.5) or Triton X-100, separated the soluble and the membrane-bound fractions by ultracentrifugation, and analyzed the distribution of RoDH-4 by western blotting. Human liver microsomal carboxylesterase hCE-1, known to reside in the lumen of the endoplasmic reticulum, was used as a control for the efficiency of extraction. These experiments showed that liver RoDH-4 remained bound to the microsomal membranes after alkaline treatment but was extracted by Triton X-100, consistent with the behavior of an integral membrane protein (Figure 3A). As an integral membrane protein, RoDH-4 could be inserted into the membrane with the polypeptide chain facing the cytosol or the lumen of the endoplasmic reticulum. If RoDH-4 was inserted facing the cytosol, it could directly bind holo-CRBP. If, on the other hand, RoDH-4 faced the lumenal side, it would require a transporter to translocate holo-CRBP across the membrane.

To determine the orientation of RoDH-4 in the membrane, we used an immunoprecipitation and glycosylation scanning approach. For immunoprecipitation, intact microsomal vesicles containing RoDH-4 were incubated with IgG against the 83 amino acid N-terminal segment or the 146 amino acid C-terminal segment of RoDH-4. Control incubations con-

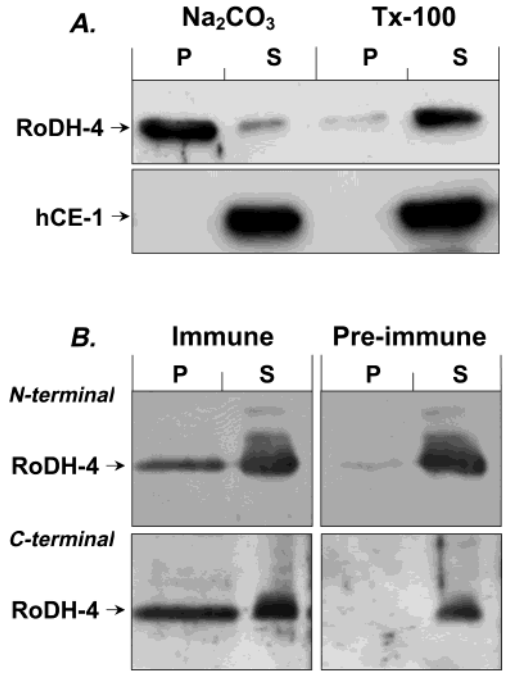

FIGURE 3: Characterization of the RoDH-4 interaction with the microsomal membranes. (A) Alkaline extraction. Human liver microsomes were extracted with sodium carbonate (Na_2CO_3) or 1% Triton X-100 (Tx-100) and centrifuged at 105000*g*. Distribution of RoDH-4 and hCE-1 between the pellet (P) and the supernatant (S) was analyzed by western blotting. (B) Immunoprecipitation of RoDH-4. Sf9 microsomes containing RoDH-4 were incubated with the N-terminal IgG at a 1:0.6 ratio (μg/μg) and with the C-terminal IgG at a 1:1 ratio (μg/μg). Control incubations contained the same amounts of the respective preimmune IgG. The mixtures were incubated overnight at 4 °C, and the immune complexes were precipitated by the addition of protein A−agarose beads. The distribution of RoDH-4 between the pellet (P) and the supernatant (S) was analyzed by western blotting. The results shown are representative of four separate experiments.

tained the respective preimmune IgG. Both the N-terminal and the C-terminal antibodies immunoprecipitated intact microsomes containing RoDH-4, whereas the preimmune sera did not (Figure 3B). Since the antibodies could bind to RoDH-4, this suggested that RoDH-4 polypeptide was exposed at the cytoplasmic surface of the microsomal membrane.

The cytosolic orientation was further confirmed by the lack of glycosylation of the RoDH-4 polypeptide. Glycosylation occurs only in the lumen of the endoplasmic reticulum and is manifested by the slower electrophoretic mobility of glycosylated proteins in SDS−PAGE. Native RoDH-4 contains a glycosylation consensus sequence NVS at Asn-161, which is not glycosylated, because liver RoDH-4 has the same electrophoretic mobility as RoDH-4 produced in vitro in the absence of microsomal membranes (Figure 4) and because treatment of human liver microsomes with Endo H does not change the electrophoretic mobility of RoDH-4 (data not shown). Furthermore, recombinant RoDH-4 polypeptides constructed to contain one, two, or three additional glycosylation consensus motifs at positions 60−62 (NLT), 124−126 (NLT), and 260−262 (NLS) were not glycosylated when expressed in Sf9 cells (Figure 4; only C60N and D260N glycosylation constructs are shown). A control protein, 11β-HSD1, was glycosylated at all three endogenous glycosylation sites (Figure 4). Thus, both immunoprecipitation and glycosylation scanning suggested that RoDH-4 faces the cytosolic side of the membrane. The cytosolic orientation of RoDH-4 would allow direct binding of the cytosolic holo-CRBP to RoDH-4.

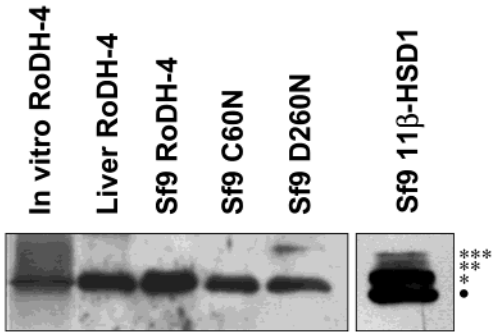

FIGURE 4: Analysis of the glycosylation state of wild-type and mutant RoDH-4. The electrophoretic mobility of ^{35}S-labeled RoDH-4 produced in vitro using a coupled transcription/translation system in the absence of microsomes (in vitro RoDH-4) was compared to that of the human liver RoDH-4 (liver RoDH-4; 5 μg of liver microsomes) and recombinant wild-type (Sf9 RoDH-4; 0.5 μg of microsomes) and mutant RoDH-4 that contained additional glycosylation sites (Sf9 C60N and Sf9 D260N; 2 μg of each microsome). Samples were separated in the same gel and transferred to a nitrocellulose filter, which was then cut in half. The filter containing ^{35}S-labeled RoDH-4 was exposed to X-ray film, whereas the second filter was hybridized with anti-RoDH-4 antibodies to visualize the microsomal RoDH-4 by chemiluminescence as described under Experimental Procedures. The two images were then aligned. 11β-HSD1 expressed in Sf9 cells (Sf9 11β-HSD1; 10 μg of microsomes) was detected by western blotting using anti-FLAG polyclonal antibodies (0.85 mg protein/mL; Sigma) at a 1:2500 dilution. Four different forms of 11β-HSD1 were observed: unglycosylated (●) and glycosylated at one (∗), two (∗∗), and three sites (∗∗∗). The second band seen in the preparation of microsomes containing the D260N mutant of RoDH-4 was due to nonspecific staining and was also observed with microsomes isolated from Sf9 cells infected with wild-type virus. This band was not removed by Endo H treatment, indicating that it was not a glycosylated form of D260N.

Purified RoDH-4 Exhibits High Catalytic Efficiency for Oxidation of Holo-CRBP. To determine the catalytic efficiency of RoDH-4 for oxidation of holo-CRBP, RoDH-4 was purified from the microsomal membranes. Previous attempts to purify microsomal retinol dehydrogenases from rat or bovine tissues using conventional methods were essentially unsuccessful. The solubilized enzymes were extremely unstable and lost almost 80% of the initial activity even at the partially purified stage (*9*, *27*−*29*). We used a different approach to purification of RoDH-4 by taking advantage of its unusual resistance to proteolysis.

We have established that human liver RoDH-4 was resistant to proteolysis at 4 °C in the presence of 1% Triton X-100 and was degraded only at higher temperature (Figure 5A). Interestingly, rat RoDH-1 was reported to exhibit similar resistance to proteolysis at low temperature (*30*). Using a coupled in vitro transcription/translation system, we found that RoDH-4 acquired its protease resistance cotranslationally in the presence of microsomal membranes, because it was completely degraded if microsomes were added after RoDH-4 protein synthesis was terminated by the addition of cycloheximide (Figure 5B). It was important to keep solubilized RoDH-4 on ice, because even brief exposures (10 min) to higher temperatures (above 15 °C) in the presence of detergents denatured RoDH-4 irreversibly, leading to com-

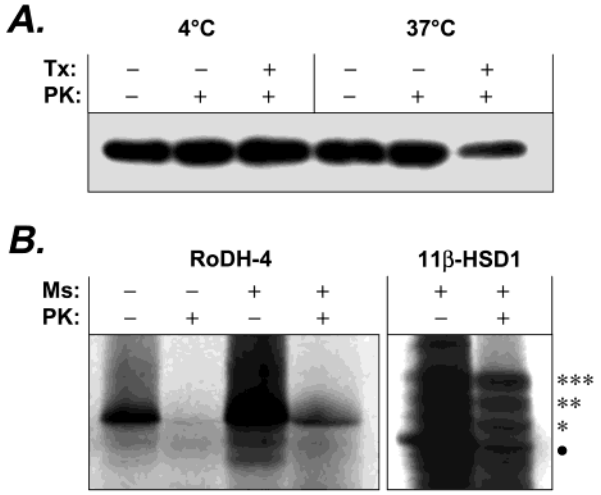

FIGURE 5: Analysis of RoDH-4 resistance to proteolysis. (A) Proteinase K digestion. Human liver microsomes (10 μg) were treated with proteinase K (PK) (1 μg) in the presence (+) or absence (−) of 1% Triton X-100 (Tx) for 1 h at 4 or 37 °C as indicated. RoDH-4 was detected by western blot analysis. RoDH-4 was completely digested after 2 h at 37 °C in the presence of Triton X-100. (B) In vitro synthesis of RoDH-4. Five hundred nanograms (0.5 μL) of linearized pT7/T3-19 plasmid containing RoDH-4 cDNA was incubated with TNT Quick master mix (10 μL) (Promega) and 10 μCi of [^{35}S]methionine (1 μL) at 30 °C. An identical reaction was performed in the presence of canine pancreas microsomes (1 μL). After 60 min, 2 mM cycloheximide was added to both tubes, followed by the addition of microsomes (1 μL) to the first tube. After an additional 30 min incubation at 30 °C, the samples were digested by 200 μg/mL proteinase K at 4 °C for 1 h. 11β-HSD1 was used as a positive control for glycosylation and protection from protease. RoDH-4 and 11β-HSD1 bands in SDS−PAGE gel were visualized by autoradiography. Four forms of 11β-HSD1 were protected from proteolysis: the translocated but not glycosylated form (●) and glycosylated at one (∗), two (∗∗), and three (∗∗∗) endogenous glycosylation sites.

Table 1: Purification of RoDH-4 from Sf9 Cells[a]

enzyme preparation	specific activity, nmol min^{-1} mg^{-1}	activity yield, %	total protein, μg	protein recovery, %	purification (*n*-fold)
microsomes	3.6	100	500	100	1.0
DHPC extract	4.0	91	410	82	1.1
DHPC extract + proteinase K	10.0	89	160	32	2.7
proteoliposomes	40.0	89	40	8	11.1

[a] The results shown are representative of five independent preparations. The specific activity of individual fractions was determined with 1 μM androsterone.

plete proteolysis of the extracted protein at 4 °C (data not shown).

To purify recombinant RoDH-4, we solubilized the membranes using mild lipid-like detergent DHPC and removed the detergent-insoluble material by ultracentrifugation. This step yielded 91% of the total microsomal RoDH-4 activity in the supernatant (Table 1 and Figure 6A, lane 2). Then, the DHPC extract was treated with proteinase K at 4 °C overnight. Under these conditions, RoDH-4 remained intact and fully active while most other Sf9 proteins were degraded (Figure 6A, lane 3). Treatment with proteinase K resulted in partial purification of RoDH-4 and played an important role during subsequent reconstitution of the digested DHPC extract into proteoliposomes. Unlike RoDH-4, most Sf9

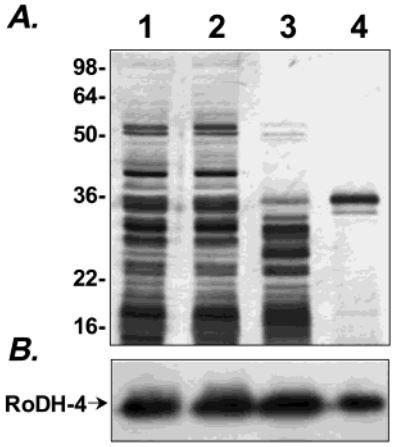

FIGURE 6: Purification and reconstitution of RoDH-4 into proteoliposomes. (A) Silver-stained SDS−PAGE. Lanes: 1, Sf9 microsomes containing RoDH-4 (9 μg); 2, DHPC extract of Sf9 microsomes (9 μg); 3, DHPC extract treated with proteinase K (10:1) for 14 h at 4 °C (4.5 μg); 4, proteoliposomes with reconstituted RoDH-4 (0.7 μg). (B) Western blot analysis of RoDH-4. Lanes 1 and 2 contained the same amount of protein as in panel A. Lane 3 contained 9 μg of DHPC extract treated with proteinase K, and lane 4 contained 0.2 μg of proteoliposomes.

proteins were degraded to such an extent that they could no longer integrate into the artificial membrane. Therefore, reconstitution into proteoliposomes was the most effective purification step of the protocol. SDS−PAGE analysis of the reconstituted proteoliposomes showed that they contained a nearly homogeneous protein band of ∼36 kDa subunit molecular mass (Figure 6A, lane 4). The protein was recognized by RoDH-4-specific antibodies (Figure 6B, lane 4), confirming that RoDH-4 integrated into the proteoliposomes. The overall activity yield was 89% of the initial RoDH-4 activity in the microsomal membranes (Table 1). The specific activity of the enzyme increased 11-fold compared to the microsomal preparation. The purification protocol was very reproducible, consistently resulting in a highly purified preparation of RoDH-4.

Reconstituted RoDH-4 resisted extraction with sodium carbonate (pH 11.5) (data not shown), as expected for an integral membrane protein properly inserted into a lipid bilayer, and remained resistant to proteolysis at 4 °C in the presence of detergent (data not shown). Sealed proteoliposomes were immunoprecipitated by RoDH-4 antibodies, consistent with the cytosolic orientation of the protein (data not shown). To determine whether all of the RoDH-4 protein integrated into the lipid bilayer with the right side out, we permeabilized proteoliposomes using a pore-forming peptide, alamethicin, to allow free translocation of NAD^+ into the lumen and assayed the activity of RoDH-4. If part of the RoDH-4 protein integrated with the lumenal orientation of the active site, we would have observed an increase in RoDH-4 activity in the presence of alamethicin. The activity of RoDH-4 in permeabilized proteoliposomes determined at 1, 3, 5, and 10 min of incubation was identical to that of the intact proteoliposomes (data not shown), indicating that all of RoDH-4 was oriented toward the cytosol. The same result was obtained for RoDH-4-containing microsomes.

Purified RoDH-4 was remarkably stable when stored in a refrigerator, retaining nearly full activity for at least 4 months after reconstitution into proteoliposomes. The apparent K_m values of purified RoDH-4 for holo-CRBP, androsterone, and

Table 2: Kinetic Constants of the Purified RoDH-4 Reconstituted into Proteoliposomes and of the Microsomal Preparation of RoDH-4[a]

substrate/ cofactor	proteoliposomes		microsomes	
	K_m, μM	V_{max}, nmol min^{-1} mg^{-1}	K_m, μM	V_{max}, nmol min^{-1} mg^{-1}
androsterone	0.20 ± 0.03	44 ± 2	0.16 ± 0.03	3.9 ± 0.3
holo-CRBP	2.7 ± 0.6	4.4 ± 0.3	3.8 ± 0.8	0.39 ± 0.03
NAD^+	0.24 ± 0.06		0.29 ± 0.14	

[a] The reactions with holo-CRBP contained 0.625 μg/mL proteoliposomes or 5.5 μg/mL microsomes and were carried out for 20 min at 37 °C. The reactions with androsterone contained 0.1 μg/mL proteoliposomes or 0.8 μg/mL microsomes and were carried out for 15 min at 37 °C. The concentration of NAD^+ was 1 mM. Kinetic constants were calculated using GraFit (Erithacus Software Ltd.) and expressed as the means ± SD.

NAD^+ agreed well with the values determined for the microsomal enzyme (Table 2). From the V_{max} value of 4.4 nmol min^{-1} mg^{-1} and the subunit molecular mass of ~35 kDa, we calculated that the k_{cat} value of the purified RoDH-4 was 0.16 min^{-1}, translating into the catalytic efficiency (k_{cat}/K_m) of 59 min^{-1} mM^{-1}. Thus, characterization of the purified RoDH-4 confirmed that it was active with holo-CRBP and did not require other proteins/transporters for its activity, consistent with the cytosolic orientation in the membrane.

Apo-CRBP Is a Competitive Inhibitor of Holo-CRBP Oxidation. Recognition of holo-CRBP as a substrate suggested that RoDH-4 had a specific binding site for CRBP. This implied that apo-CRBP could also bind to the same protein binding site on RoDH-4 and, possibly, act as a competitive inhibitor of holo-CRBP oxidation. To test this prediction, we titrated the holo-CRBP-containing reaction mixtures with an increasing amount of apo-CRBP and determined RoDH-4 activity. Apo-CRBP was a potent inhibitor of holo-CRBP oxidation. For example, 1.2 μM apo-CRBP reduced oxidation of 5 μM holo-CRBP by 67%, suggesting that RoDH-4 had a stronger interaction with the apoprotein than with the holoprotein. The inhibition of RoDH-4 activity by apo-CRBP also suggested that RoDH-4 was able to specifically recognize the apoprotein. To obtain the K_i value for apo-CRBP, we determined the rate of retinal formation by RoDH-4 at four to six concentrations of holo-CRBP as substrate in the absence or presence of apo-CRBP (0.6, 1.2, and 3.0 μM). The Lineweaver−Burk transformation of the data set showed that the inhibition was competitive with a calculated K_i value of 0.20 ± 0.03 μM. Thus, the competitive inhibition by apo-CRBP provided further evidence for the direct interaction of the binding protein with RoDH-4 and suggested that the activity of RoDH-4 is regulated at the level of the apo- to holo-CRBP ratio.

DISCUSSION

Free retinol can be oxidized to retinaldehyde by multiple dehydrogenases residing in the cytosolic as well as the microsomal compartments of the cell (*31*). The best known cytosolic retinol dehydrogenases are the multisubstrate NAD^+-dependent medium-chain alcohol dehydrogenases (ADHs) (*31*). Among ADHs, class I ADH (ADH1), highly expressed in liver and in a number of extrahepatic tissues, and class IV ADH (ADH4), expressed mainly in the epithelial lining of the stomach and esophagus, are thought to be the major contributors to the retinol oxidation by the cytosolic fraction of the cells. The catalytic efficiencies of the human ADH1 and ADH4 for oxidation of free retinol are 19 min^{-1}mM^{-1} (for $\gamma\gamma$ isozyme) (*32*) and 2600 min^{-1}mM^{-1} (*33*), respectively, with the K_m values in the upper micromolar range (9−290 μM). Besides ADH1 and ADH4, the ubiquitously expressed class III ADH (ADH3), also known as a glutathione-dependent formaldehyde dehydrogenase, was recently shown to possess a weak retinol dehydrogenase activity toward free all-*trans*-retinol (~0.105 nmol min^{-1} mg^{-1}) (*34*). However, neither ADH isozyme appears to be able to utilize holo-CRBP as substrate (*19*, *35*, *36*). Thus, the contribution of ADH enzymes to retinoic acid biosynthesis depends on the amount of free retinol in the cells.

In the liver and, presumably, other cells with a high level of CRBP, holo-CRBP appears to be the predominant form of retinol (*8*). Previous reports suggested that the bound forms of retinoids are metabolically active but can be utilized only by certain enzymes. For example, free retinol is esterified to retinyl esters by two microsomal acyltransferases, acyl-CoA:retinol acyltransferase (ARAT) and lecithin−retinol acyltransferase (LRAT) (*37*, *38*). Only LRAT recognizes the CRBP-bound form of retinol as substrate (*37*, *38*). Similarly, free retinaldehyde is oxidized to retinoic acid in vitro by both human ALDH type I and human ALDH type II (*39*), but only ALDH type I exhibits significant activity toward CRBP-bound retinaldehyde (*39*).

The results of the present study suggest that, although RoDH-4 and RoDH-like 3α-HSD exhibit similar substrate and cofactor specificity, share 65% amino acid sequence identity, and have similar genomic organization on chromosome 12 (*40*), the two human microsomal retinol/sterol dehydrogenases are not functionally equivalent in terms of their ability to utilize holo-CRBP. RoDH-like 3α-HSD is unable to access the bound form of retinol, whereas RoDH-4 exhibits significant holo-CRBP dehydrogenase activity. The recognition of holo-CRBP as substrate by RoDH-4 is especially convincing because RoDH-like 3α-HSD is actually more active toward free retinol than RoDH-4. Therefore, the level of RoDH-like 3α-HSD activity in the presence of holo-CRBP as substrate serves as a good indicator of the amount of free retinol in the reaction mixture. Lack of RoDH-like 3α-HSD activity in the presence of CRBP indicates that retinol remains bound to CRBP during the reaction and that holo-CRBP is the only available substrate. Therefore, the formation of retinaldehyde from holo-CRBP in the presence of RoDH-4 appears to be due to the direct interaction between RoDH-4 and holo-CRBP. This conclusion is in agreement with the previous report that recombinant RoDH-4 (hRDH-E) recognizes holo-CRBP as substrate (*15*).

Since holo-CRBP is localized in the cytosolic compartment of the cells and RoDH-4 is an integral membrane protein, a direct interaction between the two proteins inside the cells can occur only if RoDH-4 faces the cytosolic side of the membrane. Indeed, the results of immunoprecipitation and glycosylation scanning demonstrated that the segments of the RoDH-4 polypeptide chain that carry the cofactor-binding (36-GCDSGFG-42) and the substrate-binding (176-YCISK-180) domains are exposed at the cytosolic surface of the membrane, indicating that the catalytic site of RoDH-4 is oriented toward the cytosol. This result is consistent with

the model of RoDH-4 insertion into the membrane proposed on the basis of the analysis of the primary structure of RoDH-4 (*14*). Rat RoDH-1 was also shown to face the cytosolic side of the membrane (*30*), in agreement with binding of holo-CRBP to RoDH-1 in the presence of $NADP^+$ (*41*).

Characterization of the purified RoDH-4, stabilized by reconstitution into proteoliposomes, confirmed that RoDH-4 can utilize holo-CRBP as substrate in the absence of other proteins, consistent with the cytosolic orientation of RoDH-4. Furthermore, it provided the first opportunity to compare the catalytic efficiencies of RoDH versus ADH retinol dehydrogenases. It is now clear that the catalytic efficiency of RoDH-4 toward CRBP-bound retinol (59 min^{-1} mM^{-1}) is actually higher than the catalytic efficiency of ADH1 toward free all-*trans*-retinol (see above). It has been established that the oxidation of all-*trans*-retinol to all-*trans*-retinaldehyde is the rate-limiting step in the biosynthesis of retinoic acid (*3*). One can calculate the catalytic efficiency of the human ALDH type I, which catalyzes the second step of retinoic acid biosynthesis, oxidation of CRBP-bound retinaldehyde to retinoic acid. On the basis of the reported V_{max} value of 29 nmol min^{-1} mg^{-1}, the K_m value of 1.7 μM (*39*), and the subunit molecular mass of 56 kDa, the k_{cat} value of human ALDH type I calculates as 1.6 min^{-1} with the catalytic efficiency of 940 min^{-1} mM^{-1}. The higher k_{cat}/K_m value of ALDH type I and the lower level of RoDH-4 protein expression in the liver are consistent with the retinol oxidation being the rate-limiting step in retinoic acid biosynthesis.

It is well established that the intracellular levels of retinoic acid are tightly controlled during differentiation and development. The exact mechanisms of this regulation are not yet fully understood. The results of the present study suggest that the activity of the enzyme that utilizes holo-CRBP as substrate is highly sensitive to the inhibition by apo-CRBP. The levels of CRBP in the cells and tissues are known to vary during differentiation and development (*42*−*44*), in response to changes in cellular cAMP levels (*45*) and as a result of vitamin A deficiency or treatment with retinoic acid (*46*−*53*). The gene promoter for CRBP type I contains a functional retinoic acid response element (*54*), and treatment of cells with retinoic acid results in an increased expression of CRBP (*46*−*53*). For example, treatment of human skin with all-*trans*-retinoic acid induces CRBP mRNA expression 5.5−5.7-fold and CRBP protein 3.0−3.2-fold after 24−96 h of treatment (*51*). During vitamin A deficiency levels of CRBP mRNA and protein decrease (*48*). However, although the levels of CRBP mRNA can vary severalfold, the changes in CRBP protein in certain cells may not be as dramatic. A recent study by Eskild et al. (*55*) suggested that the level of CRBP in rat Sertoli cells is controlled at both the transcriptional and translational level. The authors observed that the rate of CRBP degradation decreased in the presence of cAMP and proposed that the cells may use attenuation of protein synthesis and degradation as a means of maintaining the desired amount of CRBP. The low K_i value of apo-CRBP for inhibition of holo-CRBP oxidation (0.2 μM) could be necessary to sense minor changes in the level of apo-CRBP in the cells. Interestingly, apo-CRBP does not appear to inhibit the oxidation of androsterone (*14*), which is consistent with the notion that apo-CRBP specifically competes with holo-CRBP for the binding site on RoDH-4 and can, therefore, modulate the rate of retinol oxidation but not of androsterone.

Inhibition by apo-CRBP might serve as a highly sensitive feedback regulation mechanism that allows the control of local levels of retinoic acid. If the level of apo-CRBP rises as a result of holo-CRBP oxidation or in response to increased retinoic acid concentration, the elevated apoCRBP/holo-CRBP ratio prevents further oxidation of holo-CRBP by RoDH-4. A similar mechanism has been proposed for the regulation of LRAT, one of the few enzymes that could compete with RoDH-4 for holo-CRBP as substrate. Microsomal preparations of LRAT esterify holo-CRBP with the apparent K_m value of ~0.78 μM and are inhibited by apo-CRBP with a K_i value of 0.21 μM (*56*). Like CRBP, LRAT is known to be regulated by retinoic acid (*56*−*59*). It was reported that induction of LRAT by retinoic acid in human skin keratinocytes reduced conversion of retinol to RA by 50% (*61*). However, a decrease in LRAT expression during vitamin A deficiency (*57*−*60*) would prevent the competition between esterification and oxidation of holo-CRBP and target retinol for oxidation. Furthermore, stimulation of retinyl ester hydrolase by accumulating apo-CRBP (*62*) would promote retinyl ester hydrolysis and saturation of CRBP with retinol to provide the substrate for retinoic acid biosynthesis.

Characterization of the retinol dehydrogenase activity of human RoDH-4 and RoDH-like 3α-HSD carried out in the present study identifies RoDH-4 as the enzyme capable of utilizing the bound form of retinol in human tissues. The holo-CRBP dehydrogenase activity of this enzyme may play a critical role in the biosynthesis of retinoic acid under conditions when holo-CRBP is the only form of retinol avaliable for oxidation.

ACKNOWLEDGMENT

We thank Dr. Kirill Popov, Division of Molecular Biology and Biochemistry, University of Missouri−Kansas City, for critique and helpful suggestions.

REFERENCES

1. Mangelsdorf, D., Umesono, K., and Evans, R. M. (1994) in *The Retinoids*: *Biology, Chemistry and Medicine* (Sporn, M. B., Roberts, A. B., and Goodman, D. S., Eds.) 2nd ed., pp 319−350, Raven Press, New York.
2. Maden, M. (2000) *Proc. Nutr. Soc. 59*, 65−73.
3. Napoli, J. L., and Race, K. R. (1987) *Arch. Biochem. Biophys. 255*, 95−101.
4. Noy, N. (2000) *Biochem. J. 348*, 481−495.
5. Vogel, S., Mendelsohn, C. L., Mertz, J. R., Piantedosi, R., Waldburger, C., Gottesman, M. E., and Blaner, W. S. (2001) *J. Biol. Chem. 276*, 1353−1360.
6. Folli, C., Calderone, V., Ottonello, S., Bolchi, A., Zanotti, G., Stoppini, M., and Berni, R. (2001) *Proc. Natl. Acad. Sci. U.S.A. 98*, 3710−3715.
7. Folli, C., Calderone, V., Ramazzina, I., Zanotti, G., and Berni, R. (2002) *J. Biol. Chem. 277*, 41970−41977.
8. Napoli, J. L. (1999) *Biochim. Biophys. Acta 1440*, 139−162.
9. Boerman, M. H., and Napoli, J. L. (1995) *Biochemistry 34*, 7027−7037.
10. Chai, X., Boerman, M. H., Zhai, Y., and Napoli, J. L. (1995) *J. Biol. Chem. 270*, 3900−3904.
11. Chai, X., Zhai, Y., Popescu, G., and Napoli, J. L. (1995) *J. Biol. Chem. 270*, 28408−28412.
12. Biswas, M. G., and Russell, D. W. (1997) *J. Biol. Chem. 272*, 15959−15966.
13. Hardy, D. O., Ge, R. S., Catterall, J. F., Hou, Y. T., Penning, T. M., and Hardy, M. P. (2000) *Endocrinology 141*, 1608−1617.

14. Gough, W. H., VanOoteghem, S., Sint, T., and Kedishvili, N. Y. (1998) *J. Biol. Chem. 273*, 19778−19785.
15. Jurukovski, V., Markova, N. G., Karaman-Jurukovska, N., Randolph, R. K., Su, J., Napoli, J. L., and Simon, M. (1999) *Mol. Genet. Metab. 67*, 62−73.
16. Chetyrkin, S. V., Hu, J., Gough, W. H., Dumaual, N., and Kedishvili, N. Y. (2001) *Arch. Biochem. Biophys. 386*, 1−10.
17. Chetyrkin, S. V., Belyaeva, O. V., Gough, W. H., and Kedishvili, N. Y. (2001) *J. Biol. Chem. 276*, 22278−22286.
18. Lowry, O. H., Rosebrough, N. H., Farr, A. L., and Randall, R. J. (1951) *J. Biol. Chem. 193*, 265−275.
19. Kedishvili, N. Y., Gough, W. H., Davis, W. I., Parsons, S., Li, T. K., and Bosron, W. F. (1998) *Biochem. Biophys. Res. Commun. 249*, 191−196.
20. Landers, G. M. (1990) *Methods Enzymol. 189*, 70−80.
21. Segel, I. H. (1975) *Enzyme Kinetics. Behavior and Analysis of Rapid Equilibrium and Steady-state Enzyme Systems*, pp 18−159, John Wiley & Sons, New York.
22. Marquart, D. W. (1963) *J. Soc. Ind. Appl. Math. 11*, 431−441.
23. Fisher, M. B., Campanale, K., Ackermann, B. L., VandenBranden, M., and Wrighton, S. A. (2000) *Drug Metab. Dispos. 28*, 560−566.
24. Brzezinski, M. R., Abraham, T. L., Stone, C. L., Dean, R. A., and Bosron, W. F. (1994) *Biochem. Pharmacol. 48*, 1747−1755.
25. Kessi, J., Poirée, J.-C., Wehrli, E., Bachofen, R., Semenza, G., and Hauser, H. (1994) *Biochemistry 33*, 10825−10836.
26. Weber, T., Zemelman, B. V., McNew, J. A., Westermann, B., Gmachl, M., Parlati, F., Sollner, T. H., and Rothman, J. E. (1998) *Cell 92*, 759−772.
27. Nicotra, C., and Livrea, M. A. (1982) *J. Biol. Chem. 257*, 11836−11841.
28. Ishiguro, S., Suzuki, Y., Tamai, M., and Mizuno, K. (1991) *J. Biol. Chem. 266*, 15520−15524.
29. Suzuki, Y., Ishiguro, S., and Tamai, M. (1993) *Biochim. Biophys. Acta 1163*, 201−208.
30. Duester, G. (2000) *Eur. J. Biochem. 267*, 4315−4324.
31. Yang, Z. N., Davis, G. J., Hurley, T. D., Stone, C. L., Li, T. K., and Bosron, W. F. (1994) *Alcohol Clin. Exp. Res. 18*, 587−591.
32. Kedishvili, N. Y., Gough, W. H., Chernoff, E. A. G., Hurley, T. D., Stone, C. L., Bowman, K. D., Popov, K. M., Bosron, W. F., and Li, T. K. (1997) *J. Biol. Chem. 272*, 7494−7500.
33. Molotkov, A., Fan, X., Deltour, L., Foglio, M. H., Martras, S., Farrés, J., Parés, X., and Duester, G. (2002) *Proc. Natl. Acad. Sci. U.S.A. 99*, 5337−5342.
34. Ong, D. E., Kakkad, B., and MacDonald, P. N. (1987) *J. Biol. Chem. 262*, 2729−2736.
35. Boerman, M. H. E. M., and Napoli, J. L. (1996) *J. Biol. Chem. 271*, 5610−5616.
36. Ong, D. E., MacDonald, P. N., and Gubitosi, A. M. (1988) *J. Biol. Chem. 263*, 5789−5796.
37. Yost, R. W., Harrison, E. H., and Ross, A. C. (1988) *J. Biol. Chem. 263*, 18693−18701.
38. Ambroziak, W., Izaguirre, G., and Pietruszko, R. (1999) *J. Biol. Chem. 274*, 33366−33373.
39. Kedishvili, N. Y., Belyaeva, O. V., and Gough, W. H. (2001) *Chem.-Biol. Interact. 130*−*132*, 457−467.
40. Wang, J., Bongianni, J. K., and Napoli, J. L. (2001) *Biochemistry 40*, 12533−12540.
41. Penzes, P., and Napoli, J. L. (1999) *Biochemistry 38*, 2088−2093.
42. Wei, L. N., Blaner, W. S., Goodman, D. S., and Nguyen-Huu, M. C. (1989) *Mol. Endocrinol. 3*, 454−463.
43. Wardlaw, S. A., Bucco, R. A., Zheng, W. L., and Ong, D. E. (1997) *Biol. Reprod. 56*, 125−132.
44. Zovich, D. C., Orologa, A., Okuno, M., Kong, L. W., Talmage, D. A., Piantedosi, R., Goodman, D. S., and Blaner, W. S. (1992) *J. Biol. Chem. 267*, 13884−13889.
45. Eskild, W., Oyen, O., Beebe, S., Jahnsen, T., and Hansson, V. (1988) *Biochem. Biophys. Res. Commun. 152*, 1504−1510.
46. Kato, M., Blaner, W. S., Mertz, J. R., Das, K., Kato, K., and Goodman, D. S. (1985) *J. Biol. Chem. 260*, 4832−4838.
47. Blaner, W. S., Das, K., Mertz, J. R., Das, S. R., and Goodman, D. S. (1986) *J. Lipid Res. 10*, 1084−1088.
48. Rajan, N., Blaner, W. S., Soprano, D. R., Suhara, A., and Goodman, D. S. (1990) *J. Lipid Res. 31*, 821−829.
49. Harada, H., Miki, R., Masushige, S., and Kato, S. (1995) *Endocrinology 136*, 5329−5335.
50. Okuno, M., Caraveo, V. E., Goodman, D. S., and Blaner, W. S. (1995) *J. Lipid Res. 36*, 137−147.
51. Fisher, G. J., Reddy, A. P., Datta, S. C., Kang, S., Yi, J. Y., Chambon, P., and Voorhees, J. J. (1995) *J. Invest. Dermatol. 105*, 80−86.
52. Whitney, D., Massaro, G. D., Massaro, D., and Clerch, L. B. (1999) *Pediatr. Res. 45*, 2−7.
53. Perozzi, G., Barila, D., Plateroti, M., Sambuy, Y., Nobili, F., and Gaetani, S. (1998) *Z. Ernaehrungswiss. 37*, 29−34.
54. Smith, W. C., Nakshatri, H., Leroy, P., Rees, J., and Chambon, P. (1991) *EMBO J. 10*, 2223−2230.
55. Eskild, W., Troen, G., Blaner, W. S., Nilsson, A., and Hansson, V. (2000) *J. Reprod. Fertil. 119*, 101−109.
56. Herr, F. M., and Ong, D. E. (1992) *Biochemistry 31*, 6748−6755.
57. Matsuura, T., Gad, M. Z., Harrison, E. H., and Ross, A. C. (1997) *J. Nutr. 127*, 218−224.
58. Zolfaghari, R., and Ross, A. C. (2000) *J. Lipid Res. 41*, 2024−2034.
59. Zolfaghari, R., and Ross, A. C. (2002) *J. Nutr. 132*, 1160−1164.
60. Zolfaghari, R., Wang, Y., Chen, Q., Sancher, A., and Ross, A. C. (2002) *Biochem. J. 368*, 621−631.
61. Kurlandsky, S. B., Duell, E. A., Kang, S., Voorhees, J. J., and Fisher, G. J. (1996) *J. Biol. Chem. 271*, 15346−15352.
62. Boerman, M. H., and Napoli, J. L. (1991) *J. Biol. Chem. 266*, 22273−22278.

BI026836R